Applied Thermal Engineering 176 (2020) 115442

Contents lists available at ScienceDirect

Applied Thermal Engineering

journal homepage: www.elsevier.com/locate/apthermeng

Adsorption characteristics and cooling/heating performance of COF-5

Xiaoxiao Xia[a,c], Zhilu Liu[a,c], Song Li[a,b,c,*]

[a] State Key Laboratory of Coal Combustion, School of Energy and Power Engineering, Huazhong University of Science and Technology, Wuhan 430074, China
[b] China-EU Institute for Clean and Renewable Energy, Huazhong University of Science and Technology, Wuhan 430074, China
[c] Nano Interface Center for Energy, School of Energy and Power Engineering, Huazhong University of Science and Technology, Wuhan 430074, China

HIGHLIGHTS

- COF-5 exhibit preferential stepwise adsorption isotherm for adsorption cooling.
- COF-5 displayed the higher COP_C than CuBTC, MIL-101(Cr), and ZIF-8.
- The higher COP of COF-5 at a wider range of temperature lift is favorable especially at low desorption temperature.

ARTICLE INFO

Keywords:
Heat pumps
Covalent-organic frameworks
Ethanol
Coefficient of performance
Temperature lift

ABSTRACT

Adsorption-driven heat pumps (AHPs) powered by low-grade waste heat and solar energy are promising to reduce the energy consumption for cooling and heating. Seeking novel high-performing adsorbents of AHPs is the key to improve their cooling/heating performance. Very recently, the potential use of covalent-organic frameworks (COFs) adsorbents of AHPs has won increasing research interests. However, the adsorption cooling/heating performance of COFs under varying working conditions is still unexplored. In this study, COF-5 was synthesized and tested to obtain the adsorption isotherms of ethanol working fluid. For comparison, three commonly used metal-organic frameworks (MOFs), including Cu-BTC, MIL-101(Cr), and ZIF-8, were also investigated. The cooling/heating performance of COF-5/ethanol and MOF/ethanol working pairs was evaluated by mathematical modelling based on the basic thermodynamic cycle of AHPs. The results demonstrated that COF-5 with the high coefficient of performance for cooling/heating (COP_C/COP_H) under wide temperature lift (ΔT_{lift}) outperformed MOFs, especially for cooling.

1. Introduction

Energy consumption for space cooling and heating expected to continuously rise results in severe global warming. In order to decrease energy consumption and carbon dioxide emission, it is crucial to mitigate primary energy requirement for cooling and heating by utilizing the waste heat or renewable solar energy [1]. Adsorption-driven heat pumps (AHPs) powered by low-grade waste heat or solar energy has attracted growing attention as a sustainable alternative to vapor compression heat pumps [2,3]. However, AHPs based on conventional working pairs including silica gel/water [4], zeolite/water [5] and activated carbon/ammonia [6] usually exhibit low adsorption capacity and/or require high regeneration temperature, leading to an unsatisfactory coefficient of performance (COP) that is unfavorable for the wide application of AHPs [7,8]. Seeking high-performing working pairs especially adsorbents has been a crucial strategy to improve the performance of AHPs [9].

In recent decades, a series of novel porous materials such as metal-organic frameworks (MOFs) have been used for AHPs. MOFs have been recognized as potential adsorbent candidates for AHPs because of their ultra-high surface area and large pore volume [10]. Water is the most commonly used working fluid for AHPs due to their environment-friendliness and abundance in nature. It has been reported that CAU-10(Al)/water [11] can be efficiently used (COP_C = 0.72) for wide temperature lift (T_{lift} = 26 K) at T_{des} = 373 K and T_{ads} = T_{con} = 303 K for cooling [12]. MIL-101(Cr)/water working pair was recognized as potential candidates for AHPs, whose COP_C can reach 0.89 at T_{des} = 373 K and T_{con} = 303 K [13], due to the high water uptake (up to 1.6 g/g) and water stability of MIL-101(Cr) [14]. UiO-66/water has been reported as a promising working pair due to the high specific cooling effect (SCE = 820 kJ/kg) and COP_C (COP_C = 0.86) for cooling (T_{ads} = T_{con} = 303 K, T_{eva} = 295 K, T_{des} = 343 K) [15]. However,

* Corresponding author.
E-mail address: songli@hust.edu.cn (S. Li).

https://doi.org/10.1016/j.applthermaleng.2020.115442
Received 1 December 2019; Received in revised form 8 April 2020; Accepted 3 May 2020
Available online 05 May 2020

Nomenclature

Symbols

COP	coefficient of performance
C_p	specific heat capacity (kJ/kg)
LH	latent heat (kJ/kg)
P	pressure (Pa)
P_0	saturation pressure (Pa)
Q	heat transfer (kJ/kg)
q_{st}	isosteric heat of adsorption (kJ/mol)
R	ideal gas constant (J/mol·K)
SCE	specific cooling effect (kJ/kg)
SHE	specific heating effect (kJ/kg)
T	temperature (K)

Subscripts

ads	adsorption
C	cooling
con	condensation
des	desorption
eva	evaporation
H	heating
regen	regeneration
sorbent	adsorbent
wf	working fluid

many MOFs are not stable upon exposure to water vapor [16] such as Cu-BTC and MOF-74-Mg, both of which exhibit the high water uptake (i.e. 0.49 cm^3/g for Cu-BTC and 0.62 cm^3/g for MOF-74-Mg at 80% relative humidity). A significant loss in Brunauer-Emmett-Teller (BET) surface area was observed for both Cu-BTC and MOF-74-Mg (26% for Cu-BTC and 83% for MOF-74-Mg, respectively) after one cycle water vapor adsorption at 298 K [17]. The family of zeolitic imidazolate frameworks (ZIFs) [18] and Zr-based MOFs [19] exhibit remarkable stability in water vapor [16]. ZIF-8 has exceptionally high water stability but displays no water uptake until 80% relative humidity because of its strong hydrophobicity [20].

Compared to water, alcohols (i.e. methanol and ethanol) as working fluids exhibiting the higher vapor pressures with faster mass transfer can work at subzero temperatures [21]. Activated carbon is frequently used for adsorbing ethanol and the adsorption performance of activated carbon/ethanol working pairs has been widely investigated [22,23]. However, the COP of activated carbon/ethanol working pair is low, which cannot be used for ice making under solar energy [24]. The new family of composites, such as LiBr/silica gel [25] and salt inside porous matrix (CSPM) composites [26] with ethanol as a refrigerant has also been used for cooling with the optimum COP_C of 0.72 [25], which can be further improved by adjusting the slat types and ratios in composites. Moreover, the stability of MOFs toward alcohols is less of an issue than water [27]. Cu-BTC has been reported to exhibit higher stability for alcohols [28] and higher ethanol uptake than commonly used adsorbents such as silica gel RD (0.3 g/g for Cu-BTC *vs.* 0.2 g/g for Silica gel RD) [29]. MIL-101(Cr)/ethanol [29,30] and ZIF-8/ethanol [27] working pairs have demonstrated to be the potential candidates of AHPs. COP_C of both MIL-101(Cr) and ZIF-8 can achieve 0.65 at cooling condition (T_{ads} = 303 K, T_{eva} = 278 K), whereas the required desorption temperature of MIL-101(Cr) (T_{des} = 360 K) is slightly higher than that of ZIF-8 (T_{des} = 355 K). ZIF-8/ethanol also exhibited the wide temperature lift (35 K), which can be used for efficient ice making (T_{des} = 373 K and T_{con} = 298 K).

Our recent computational screening studies on MOFs for basic AHPs [31] and MOFs/covalent-organic frameworks (COFs) for cascaded AHPs [32] have demonstrated that the stepwise adsorption isotherms are preferential for high-performance AHPs, from which COFs [33], an emerging class of porous adsorbents consisting of fully organic unit were recognized as potential adsorbents for cooling. Experimental investigation also demonstrated that the COF TpPa-1 displayed remarkably high water uptake of 0.45 g/g, and the COP_C of TpPa-1/water working pair was able to achieve 0.77 under a low regeneration temperature of 338 K, which is comparable to the high-performing MOFs [34]. Besides, the majority of COFs were composed of organic units exhibited weak interaction towards ethanol, leading to stepwise ethanol adsorption isotherm that favors the COP_C. In addition, COFs overcome the unsatisfactory stability of most MOFs because of the instability coordination bonds between the metal ions and organic ligands of MOFs [35]. Thus, COFs may be a better alternative to MOFs that are able to meet the requirements for high-performing adsorbents in AHP systems.

However, until now, the adsorption cooling/heating performance of COFs under varying operation conditions is still an unexplored topic, especially compared with MOFs. Therefore, in this work, one of the firstly reported COFs, COF-5, and three promising MOFs in AHPs, including Cu-BTC, MIL-101(Cr), and ZIF-8, were chosen for synthesis and characterization. Their adsorption cooling and heating performance under varying working conditions were then assessed by mathematical modeling based on the measured ethanol adsorption isotherms.

2. Methodology

2.1. Experimental

Materials. All chemicals were purchased from commercial sources and used without any further purification. 2,3,6,7,10,11-hexahydroxytriphenylene (HHTP, 96%) was purchased from Zhengzhou Alfachem Co., Ltd. 1,4-benzenediboronic acid (BDBA, 97%), copper nitrate trihydrate ($Cu(NO_3)_2{\cdot}3H_2O$, 99%), trimesic acid (H_3BTC, 97%), terephthalic acid (H_2BDC, 99%), 2-methyl imidazole (98%), zinc nitrate hexahydrate ($Zn(NO_3)_2{\cdot}6H_2O$, 99%), dioxane (99%), and mesitylene (97%) were from Shanghai Aladdin Bio-Chem Technology Co., Ltd. Zirconium chloride ($ZrCl_4$, 99.95%) was purchased from J&K China Chemical Ltd. Methanol, acetone, absolute ethanol, N,N-dimethylformamide (DMF), and glacial acetic acid were from Sinopharm Chemical Reagent Co., Ltd. (AR). Nitrogen (N_2, 99.999%) and helium (He, 99.999%) gases were obtained from Huaerwen Industrial Co., Ltd.

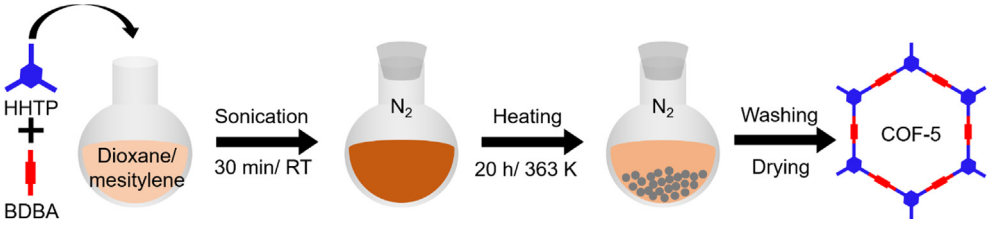

Scheme 1. Synthesis process of COF-5.

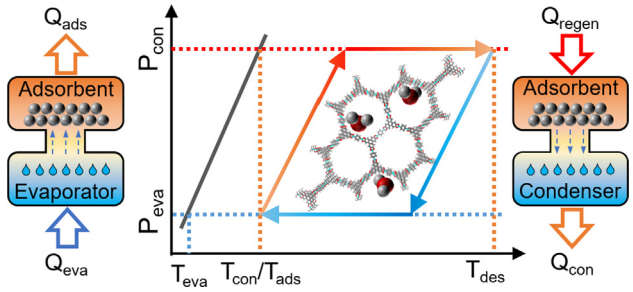

Fig. 1. Thermodynamic cycle of adsorption heat pump based on covalent-organic frameworks.

2.2. Synthesis

The selected COFs and MOFs were synthesized using a previously reported protocol with slight modification [36–39].

COF-5. HHTP (112 mg, 0.345 mmol), BDBA (86 mg, 0.52 mmol) and methanol (0.21 mL, 5.2 mmol) were added in a dioxane/mesitylene mixture solution (4:1 v/v, 43 mL) at room temperature and sonicated for 30 min under N_2 atmosphere. Then, the solution was transferred to a round bottom flask (100 mL) and heated at 363 K for 20 h in an oil-bath oven with stirring under atmospheric pressure (N_2). After cooling to room temperature, the gray solid was isolated by centrifugation and washed with acetone (30 mL × 3). Subsequently, the solid was dried under vacuum at room temperature for 12 h. The synthesis scheme of COF-5 is provided in Scheme 1.

Cu-BTC. $Cu(NO_3)_2{\cdot}3H_2O$ (3.38 g, 14 mmol) was dissolved in deionized water (75 mL). H_3BTC (2.94 g, 14 mmol) was dissolved in ethanol (75 mL) and mixed with the prepared $Cu(NO_3)_2$ solution. The mixture was placed in a 500 mL Teflon-lined autoclave and heated at 383 K for 18 h. After that, the autoclave was cooled down to room temperature and the blue solid was centrifuged and washed with deionized water (30 mL × 3). Then, the obtained solid was dried overnight at 353 K in air.

MIL-101(Cr). $Cr(NO_3)_3{\cdot}9H_2O$ (4.00 g, 10 mmol) and H_2BDC (1.66 g, 10 mmol) were added in deionized water (50 mL), followed by glacial acetic acid (0.58 mL). After that, the mixture was sonicated for 30 min at room temperature. Then the mixture was transferred into a 100 mL Teflon-lined autoclave and heated at 493 K for 8 h. After cooling to room temperature, the green solid was washed successively with deionized water, DMF and ethanol (30 mL × 3). Finally, the obtained solid was dried overnight at 423 K under vacuum.

ZIF-8. 2-methyl imidazole (1.36 g, 16.53 mmol) was dissolved in methanol (50 mL). $Zn(NO_3)_2{\cdot}6H_2O$ (1.23 g, 4.13 mmol) was dissolved in another methanol (50 mL), and then slowly added into the former solution. The mixed solution was stirred for 2 h and a milk-like suspension was formed. Afterwards, the suspension was maintained at room temperature for 24 h at static conditions. Next, the white solid was isolated by centrifugation, followed by washing with methanol (30 mL × 3). Finally, the precipitate was dried in air at room temperature for 5 h, and then dried at 453 K for 24 h in a vacuum oven.

2.3. Characterization

Powder X-ray diffraction (PXRD) data were collected on a PANalytical X'Pert X-ray diffractometer in reflection mode using Cu Kα (λ = 1.540598 Å) radiation at 1600 W (40 kV, 40 mA). The 2θ ranges from 5° to 50° (2–15° for COF-5 and MIL-101(Cr)) as a continuous scan with a step size of 0.01313° at room temperature. **N_2 adsorption isotherms** were measured at 77 K on an Autosorb-iQ2 from Quantachrome Instruments. All samples were activated at 393 K for 24 h under vacuum before measurement. Brunauer-Emmett-Teller (BET) surface areas, total pore volumes, and pore widths were determined by fitting respective models to the collected N_2 adsorption isotherms.

2.4. Adsorption isotherms measurement

Ethanol vapor adsorption isotherms were measured at 288 K and 298 K, respectively, on an Autosorb-iQ2 from Quantachrome Instruments. Absolute ethanol was added into the vapor generator as the vapor source. Prior to measurement, approximately 100 mg of samples were activated at 393 K for 24 h under vacuum. Adsorption isotherms were collected from P/P_0 = 0.01 to 0.9. P_0 represents the saturation pressure of ethanol vapor at each working temperature.

2.5. Mathematical modelling

A universal adsorption isotherm model [40] was used to fit the measured adsorption isotherms, according to which the equilibrium uptake of COF-5 and MOFs at various temperatures can be predicted.

Thermodynamic relation between pressure, temperature, and concentration of typically ideal cooling/heating cycle was depicted in Fig. S1. The basic thermodynamic figure of AHPs was used to calculate the cooling/heating performance of adsorption working pairs. COP is defined as the useful energy output divided by energy required as input. SCE/SHE is the energy that has been transferred for cooling/heating by working fluid. For cooling, [15]

$$COP_C = \frac{Q_{eva}}{Q_{regen}} = \frac{SCE}{Q_{regen}} \tag{1}$$

$$SCE = \Delta W \times LH_{T_{eva}} \tag{2}$$

$$LH_{T_{eva}} = -1.642 \times (T_{eva} - 273) + 985.7 \tag{3}$$

Here, Q_{eva} is the energy taken up in the evaporator, Q_{regen} is the energy required for the regeneration of the adsorbent (Fig. 1). To determine the required energy for the regeneration, the heat capacity of the working fluid (C_p^{wf} = 2.7 kJ/kg·K) and the adsorbent ($C_p^{sorbent}$ = 1 kJ/kg·K [41]) are used. ΔW is the working capacity that is defined as the difference between the maximum and minimum uptake ($W_{max} - W_{min}$) of working fluid, and $LH_{T_{eva}}$ is the latent heat of working fluids at evaporation temperature (T_{eva}).

For heating,

$$COP_H = \frac{Q_{con} + Q_{ads}}{Q_{regen}} = \frac{SHE}{Q_{regen}} \tag{4}$$

$$SHE = Q_{ads} + \Delta W \times LH_{T_{con}} \tag{5}$$

$$LH_{T_{con}} = -1.642 \times (T_{con} - 273) + 985.7 \tag{6}$$

Here, Q_{con} is the energy released during condensation, Q_{ads} is the energy released during the adsorption (Fig. 1), $LH_{T_{con}}$ is the latent heat of working fluids at condensation temperature (T_{con}).

Moreover, the isosteric heat of adsorption (q_{st}) is an important parameter for calculating COP. The q_{st} was calculated using the measured adsorption isotherms at two different temperatures (288 K and 298 K) according to the Clausius–Clapeyron equation (Eq. (7)).

$$q_{st} = -R\frac{\partial(\ln P)}{\partial(1/T)} \tag{7}$$

In practice, adsorption temperature (T_{ads}) equals to T_{con}, which is dependent on the ambient temperature. Here, T_{con} is set to 303 K and 318 K based on the typical summer and winter working conditions reported previously [12,42,43]. T_{eva} could depend on the applications of working pairs, and the desorption temperature (T_{des}) is determined by the temperature of heat sources. T_{eva} and T_{des} can be independently varied to find an optimum COP and SCE/SHE, as will be discussed in detail. For different applications, the operational temperatures are listed in Table 1. More detailed information can be found in Supplementary Information.

Table 1
Operational temperatures for cooling and heating.

	T_{ads} (K)	T_{con} (K)	T_{des} (K)	T_{eva} (K)
Cooling	303	303	335–395	275–295
Heating	318	318	365–425	280–300

3. Result and discussion

According to the PXRD patterns in Fig. 2, the experimental PXRD patterns perfectly matched with the simulated ones, suggesting the successful synthesis of COF-5 and MOFs. Although the hydrothermal stability of COF-5 was unsatisfied [44]., COF-5 was stable in ethanol vapor according to the location of peaks in PXRD patterns after ethanol adsorption (Fig. S2). The measured structure properties including BET surface area, total pore volume and pore width that are essential for adsorption performance of COF-5 and MOFs were summarized in Table 2. MIL-101(Cr) exhibited the highest BET surface area (3358 m^2/g) followed by COF-5 (1943 m^2/g), Cu-BTC (1831 m^2/g), and ZIF-8 (1730 m^2/g). Similarly, the total pore volumes of four materials were in the same order to their BET surface area. MIL-101(Cr) and COF-5 had a larger pore width than other selected MOFs. The largest pore volume of MIL-101(Cr) (2.09 cm^3/g) was attributed to the presence of a large fraction of mesopores in MIL-101(Cr). In terms of the isosteric heat of adsorption (q_{st}), q_{st} of COF-5 was 37.1 kJ/mol, which is obviously lower than the evaporation enthalpy of ethanol (42 kJ/mol) and q_{st} of MOFs, implicating the weak interaction between COF-5 and ethanol. The weak host-adsorbate interaction plus the large pore width of COF-5 suggested the high possibility of stepwise adsorption in COF-5, which is favorable for the adsorption cooling/heating efficiency of AHPs [2,45].

A stepwise adsorption isotherm with a steep uptake step is dynamically preferential for AHPs since the slight change in pressure leads to remarkably change in working fluid uptakes [2,45]. Canivet et al. defined α as the step position of adsorption isotherms, which is the relative pressure at which one half of the maximum uptake is reached [46]. Jeremias et al. demonstrated that $0.05 < \alpha < 0.4$ was preferred for a reasonable temperature lift and low desorption temperature [47]. Aristov reported that $0.1 < \alpha < 0.3$ was favorable for low desorption temperature [2]. According to Fig. 3, COF-5, MIL-101(Cr) and ZIF-8 shown the favorable adsorption steps of $\alpha = 0.22$, $\alpha = 0.2$ and $\alpha = 0.12$, respectively. In contrast, Cu-BTC exhibited type I adsorption isotherm ($\alpha = 0.01$), implicating the requirement of high desorption temperature, which is unfavorable for AHPs. Among the adsorbents, MIL-101(Cr) exhibited the highest ethanol uptake (0.78 g/g) at $P/P_0 = 0.9$ followed by COF-5 (0.54 g/g), Cu-BTC (0.42 g/g), and ZIF-8 (0.34 g/g), which is in the same order to their BET surface area and total pore volume. In order to comprehensively assess the cooling/heating performance of these adsorbents, their SCE/SHE and COP were computed at varying operational conditions.

3.1. Cooling performance

The variation of SCE as a function of evaporation and desorption temperature was presented in Fig. 4, from which the SCE of COF-5 was enhanced upon the increase of evaporation and desorption temperature until a plateau. Compared with MOFs, SCE of COF-5 was generally higher throughout the variation of evaporation and desorption temperatures, implicating that COF-5/ethanol working pair is able to transfer the larger amount of thermal energy for cooling at a wide range of evaporation and desorption temperatures. However, SCE of Cu-BTC was extremely low, especially at low evaporation and desorption temperatures, which was unfavorable for cooling. On the contrary, MIL-101(Cr) exhibited the highest SCE of approximately 600 kJ/kg at high evaporation and desorption temperatures. Besides, the SCE of MIL-101(Cr) was extremely sensitive to temperature variation, whereas the SCE of Cu-BTC was highly dependent on desorption temperature, similar to the SCE of ZIF-8. However, the SCE of ZIF-8 was low in most cases. Among all adsorbents, COF-5 achieved the maximum SCE (295 kJ/kg) at $T_{eva} = 295$ K and $T_{des} = 395$ K, which was higher than that of Cu-BTC (258 kJ/kg at $T_{eva} = 295$ K and $T_{des} = 395$ K) and ZIF-8 (247 kJ/kg at $T_{eva} = 295$ K and $T_{des} = 395$ K), but lower than the maximum SCE (584 kJ/kg at $T_{eva} = 295$ K and $T_{des} = 395$) of MIL-101(Cr). The moderate SCE of COF-5 can be attributed to its relatively low ΔW at specified operational conditions (Fig. S3).

Compared with SCE, both evaporation and desorption temperatures imposed significant impacts on COP_C of working pairs. High evaporation temperature directly favors COP_C due to the increased energy taken up by the evaporator. High desorption temperature is also beneficial for the higher working fluid uptake (ΔW) and thus higher cooling capacity. However, high desorption temperature will not benefit COP_C given the increased energy consumption on adsorbent regeneration. Therefore, the evaporation and desorption temperatures for the COP_C was optimized as shown in Fig. 5. As a result, COF-5 exhibited the highest COP_C ($COP_C > 0.8$) at a wide range of evaporation and desorption temperatures (Fig. 5a) compared with MOFs. The maximum COP_C ($COP_C = 0.98$) of COF-5 was achieved at $T_{eva} = 295$ K and $T_{des} = 336$ K, followed by ZIF-8 ($COP_C = 0.74$ at $T_{eva} = 295$ K and $T_{des} = 356$ K), MIL-101(Cr) ($COP_C = 0.68$ at $T_{eva} = 295$ K and $T_{des} = 343$ K), and Cu-BTC ($COP_C = 0.51$ at $T_{eva} = 295$ K and $T_{des} = 395$ K). Although MIL-101(Cr) has a high SCE owing to its ethanol uptake (Fig. 3), MIL-101(Cr) is not competitive due to its low COP_C. Overall, it was demonstrated that COF-5 can be a more potential adsorbent for adsorption cooling with high COP_C and moderate SCE.

Except for SCE and COP_C, temperature lift (ΔT_{lift}) that describes the temperature gain for cooling/heating, or the achievable temperature changes under varying working conditions was commonly adopted for assessing the performance of AHPs. Here, the temperature lift is defined as the difference between T_{con} and T_{eva}. The high temperature lift without compensating the COP_C was preferential for high-performing AHPs. The correlation between ΔT_{lift} and COP_C at varying desorption temperatures was shown in Fig. 6, from which COF-5 achieved the highest COP_C among the four adsorbents throughout the temperature lift of 8–26 K regardless of desorption temperature. The discrepancy in COP_C of COF-5 and MOFs was enlarged with increase of desorption temperature. According to the adsorption isotherms, the Q_{regen} of COF-5 can be significantly increased, whereas ΔW of Cu-BTC (Fig. S3) can be obviously enhanced with the increase of desorption temperature. Thus, COF-5 is suitable for low desorption temperature that gains a high temperature lift with excellent COP_C. Besides, the COP_C of COF-5 was

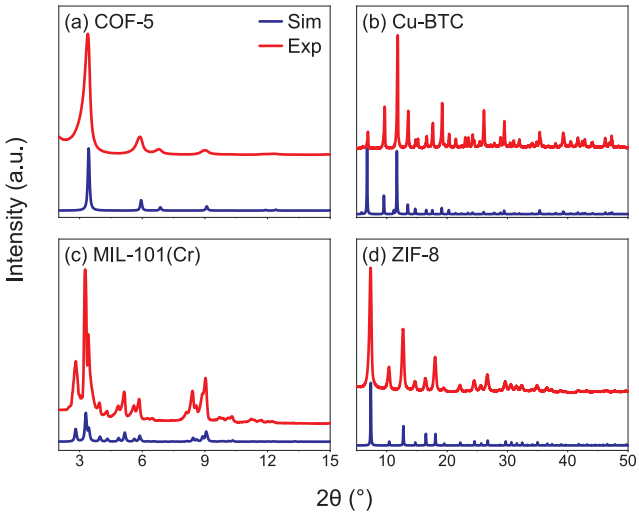

Fig. 2. Experimental (red) and simulated (blue) PXRD of (a) COF-5, (b) Cu-BTC, (c) MIL-101(Cr) and (d) ZIF-8.

Table 2
BET surface area, total pore volume, pore width and isosteric heat of adsorption (q_{st}) of COF-5, Cu-BTC, MIL-101(Cr) and ZIF-8.

Adsorbents	BET surface area (m^2/g)	Total pore volume (cm^3/g)	Pore width (nm)	q_{st} (kJ/mol)
COF-5	1943	1.23	2.58	37.1
Cu-BTC	1831	0.84	0.67	68.7
MIL-101(Cr)	3358	2.09	2.58/3.12	58.4
ZIF-8	1730	0.78	0.54	47.4

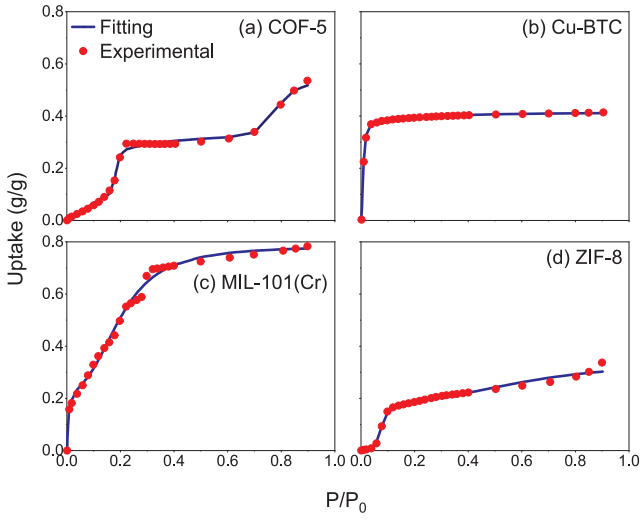

Fig. 3. Ethanol adsorption isotherms of (a) COF-5, (b) Cu-BTC, (c) MIL-101(Cr) and (d) ZIF-8 obtained from experimental measurement at 298 K (in red dots) and the fitting by the universal adsorption model (in blue lines). P_0 is the saturation pressure of ethanol vapor at 298 K.

almost constant with the increase of temperature lift until ΔT_{lift} = 25 K. Similarly, the COP_C of MIL-101(Cr), ZIF-8, and Cu-BTC was slightly reduced with ΔT_{lift}, especially at high desorption temperature (T_{des} = 395 K and 365 K). At low desorption temperature (T_{des} = 335 K), the remarkable decrease in COP_C with the increase of temperature lift was observed for all adsorbents due to the decreased ΔW (Fig. S3) at low evaporation temperature. In general, both high COP_C and wide temperature lift can be maintained by using COF-5 when ΔT_{lift} < 26 K, suggesting the potential of COF-5 for adsorption cooling.

3.2. Heating performance

Similar to SCE, SHE was enhanced with the increase of evaporation and desorption temperatures (Fig. 7). The SHE of COF-5 exhibited a steep increase at T_{eva} = 290 K, and achieved a plateau above 290 K. Whereas SHE of Cu-BTC shown significant dependence on the desorption temperature. MIL-101(Cr) shown the increasing SHE especially with the evaporation temperature and its SHE was higher than that of Cu-BTC and COF-5 due to the higher ethanol uptake of MIL-101(Cr). SHE of ZIF-8 was the lowest, which was rarely affected by the evaporation and desorption temperature. Such tendencies were in accordance with the variation of ΔW (Fig. S4). Among all adsorbents, MIL-101(Cr)/ethanol was the most promising working pair for heating with the maximum SHE of 1411 kJ/kg, followed by Cu-BTC (990 kJ/kg), COF-5 (618 kJ/kg), and ZIF-8 (524 kJ/kg) at T_{eva} = 300 K and T_{des} = 425 K.

Nevertheless, from the perspective of COP_H, COF-5 is more competitive. Throughout the variation of evaporation and desorption temperature, COP_H of COF-5 was significantly enhanced with the increase of temperature, especially evaporation temperature (Fig. 8). Similarly, COP_H of COF-5 was highly dependent on the evaporation temperature, which was above 1.6 at T_{eva} > 291 K. COP_H of Cu-BTC remarkably depended on the desorption temperature and rarely affected by evaporation temperature. In contrast, the COP_H of both MIL-101(Cr) and

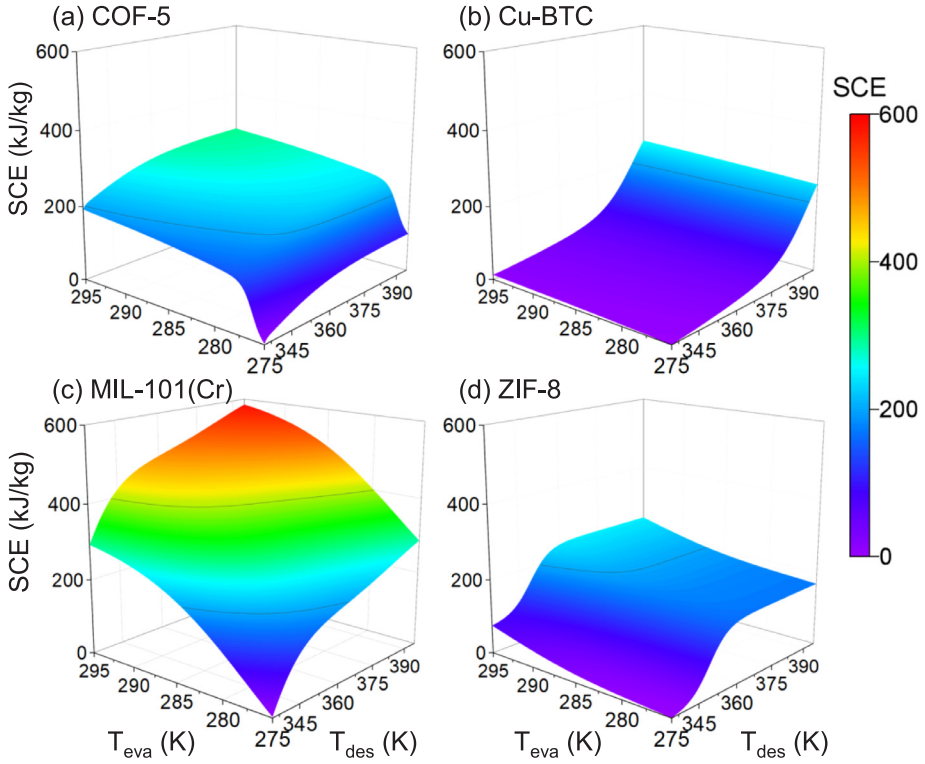

Fig. 4. SCE of (a) COF-5 (b) Cu-BTC, (c) MIL-101(Cr) and (d) ZIF-8 as a function of evaporation and desorption temperatures at given adsorption/condensation temperatures (T_{ads} = T_{con} = 303 K).

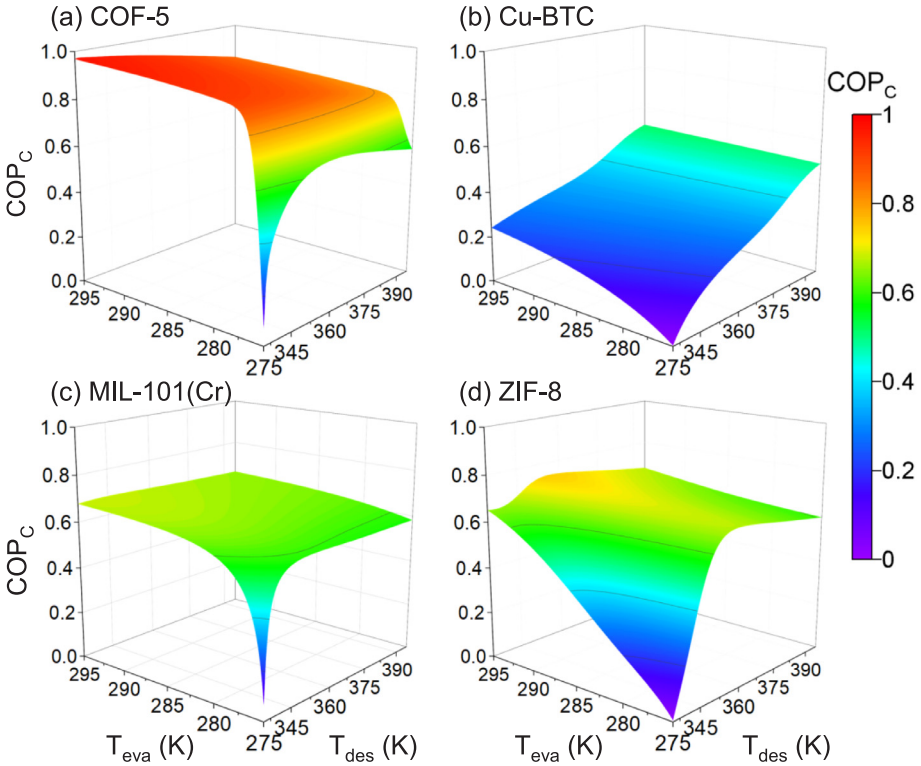

Fig. 5. COP_C of (a) COF-5 (b) Cu-BTC, (c) MIL-101(Cr) and (d) ZIF-8 as a function of evaporation and desorption temperatures at given adsorption/condensation temperatures (T_{ads} = T_{con} = 303 K).

ZIF-8 were nearly constant throughout the variation of evaporation and desorption temperature. Generally, COF-5 shown the highest COP_H of 1.79 (at T_{eva} = 300 K and T_{des} = 365 K) followed by ZIF-8 (COP_H = 1.61 at T_{eva} = 300 K and T_{des} = 376 K), MIL-101(Cr) (COP_H = 1.56 at T_{eva} = 300 K and T_{des} = 365 K), and Cu-BTC (COP_H = 1.44 at T_{eva} = 300 K and T_{des} = 425 K), implicating the potential of COF-5 for adsorption heating.

The correlation between the temperature lift and COP_H of all adsorbents for heating is more complicated than the cooling (Fig. 9). Decreased COP_H with increased temperature lift was observed for all adsorbents except Cu-BTC at T_{des} = 395 K (Fig. 9b), which can be ascribed to the increased working capacity of Cu-BTC with evaporation temperature (T_{eva}) at given T_{des} = 395 K (Fig. S5). Moreover, COF-5 outperformed MOFs at low temperature lift (ΔT_{lift} < 29 K) regardless of desorption temperatures, implicating the great potential of COF-5 for adsorption heating with low temperature lift. With the decrease of the desorption temperature, the difference in COP_H of COF-5 and other MOFs (i.e. Cu-BTC, MIL-101(Cr) and ZIF-8) was enlarged, and the COP_H of COF-5 was significantly increased at low desorption temperature, implicating the applicability of COF-5 for AHPs driven by low-temperature heat sources. Beyond ΔT_{lift} = 29 K, COP_H of COF-5 was suddenly decreased, even lower than MOFs, implicating that ΔT_{lift} of COF-5 for adsorption heating was restricted within 29 K. When ΔT_{lift} > 29 K is required, MIL-101(Cr) and ZIF-8 are more suitable candidates without remarkably compromised COP_H, especially at high desorption temperatures (T_{des} = 425 K and 395 K). Therefore, COF-5 is a suitable adsorbent for heating within the limited temperature lift compared with MOFs, especially under low desorption temperature.

4. Conclusions

Adsorption cooling and heating performance of COF-5 were investigated and compared with three commonly used MOFs including Cu-BTC, MIL-101(Cr), and ZIF-8, for the first time by integrated experimental measurement and mathematical modeling. The stepwise adsorption isotherms of COF-5 resulting from the weaker interaction between COF-5 and ethanol working fluids are favorable for adsorption cooling compared with MOFs. It was revealed that COF-5 exhibited the highest COP_C (COP_C = 0.98) among four adsorbents as well as the large temperature lift, which is favorable for adsorption cooling regardless of

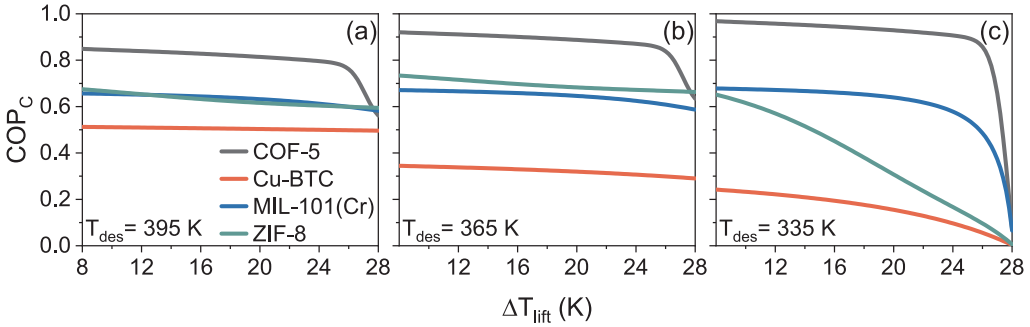

Fig. 6. COP_C of COF-5 (black), Cu-BTC (red), MIL-101(Cr) (blue) and ZIF-8 (green) as a function of temperature lift (ΔT_{lift}), obtained by varying T_{eva} when (a) T_{des} = 395 K, (b) T_{des} = 365 K and (c) T_{des} = 335 K at given condensation temperatures (T_{con} = 303 K).

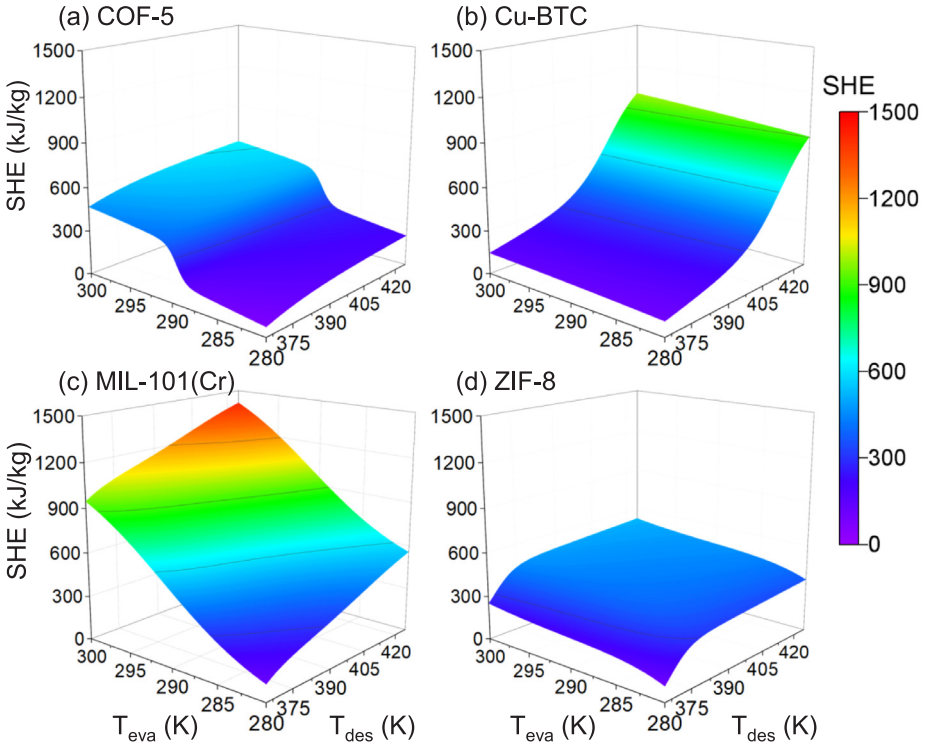

Fig. 7. SHE of (a) COF-5 (b) Cu-BTC, (c) MIL-101(Cr) and (d) ZIF-8 as a function of evaporation and desorption temperatures at given adsorption/condensation temperatures (T_{ads} = T_{con} = 313 K).

its moderate SCE. In perceptive of adsorption heating, although the COP_H of COF-5 is the highest (COP_H = 1.79) among all adsorbents, the limited temperature lift restricts its application for high temperature lift requirements. In addition, the discrepancy in both COP_C and COP_H of COF-5 and MOFs is increased with the reduction of desorption temperature, implicating the high applicability of COF-5 for low-temperature heat sources. Besides, although the cost of COF-5 in laboratory is currently high (approximately $25 per gram), it is expected to decrease with the development of large-scale production techniques. Overall, this work opens up the possibility of using covalent-organic

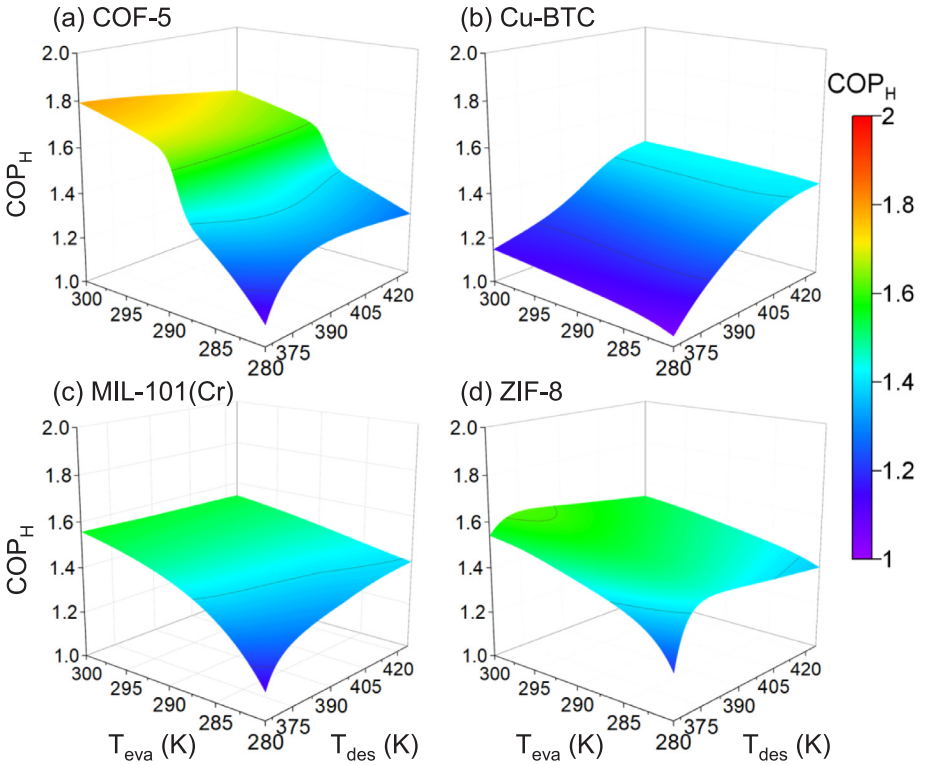

Fig. 8. COP_H of (a) COF-5 (b) Cu-BTC, (c) MIL-101(Cr) and (d) ZIF-8 as a function of evaporation and desorption temperatures at given adsorption/condensation temperatures (T_{ads} = T_{con} = 313 K).

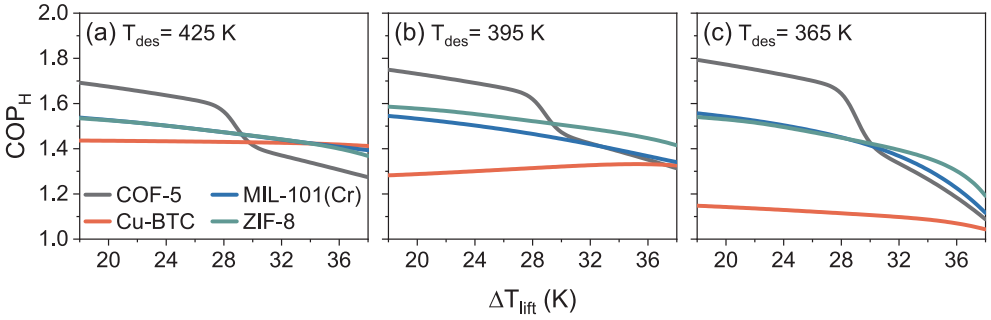

Fig. 9. COP_H of COF-5 (black), Cu-BTC (red), MIL-101(Cr) (blue) and ZIF-8 (green) as a function of temperature lift (ΔT_{lift}), obtained by varying T_{eva} when (a) T_{des} = 425 K, (b) T_{des} = 395 K and (c) T_{des} = 365 K.

frameworks (COFs) as potential adsorbents for adsorption cooling and heating under varying working conditions.

Declaration of Competing Interest

The authors declare that they have no known competing financial interests or personal relationships that could have appeared to influence the work reported in this paper.

Acknowledgement

This work was supported by Hubei Provincial Nature Science Foundation (No. 2019CFB456), National Natural Science Foundation of China (NSFC) (No. 51606081) and Double First-Class Research Funding of China-EU Institute for Clean and Renewable Energy (No. ICARE-RP-2018-HYDRO-001). This work was carried out at National Supercomputer Center in Shenzhen. We also thank Huazhong University of Science and Technology Analytical & Testing Center for providing support on material characterization.

Appendix A. Supplementary material

Supplementary data to this article can be found online at https://doi.org/10.1016/j.applthermaleng.2020.115442.

References

[1] M. Isaac, D.P. van Vuuren, Modeling global residential sector energy demand for heating and air conditioning in the context of climate change, Energy Policy 37 (2009) 507–521.
[2] Y.I. Aristov, Challenging offers of material science for adsorption heat transformation: a review, Appl. Therm. Eng. 50 (2013) 1610–1618.
[3] H. Demir, M. Mobedi, S. Ülkü, A review on adsorption heat pump: problems and solutions, Renew. Sustain. Energy Rev. 12 (2008) 2381–2403.
[4] D. Wang, J. Zhang, X. Tian, D. Liu, K. Sumathy, Progress in silica gel–water adsorption refrigeration technology, Renew. Sustain. Energy Rev. 30 (2014) 85–104.
[5] A. Myat, N. Kim Choon, K. Thu, Y.D. Kim, Experimental investigation on the optimal performance of Zeolite–water adsorption chiller, Appl. Energy 102 (2013) 582–590.
[6] Z. Tamainot-Telto, S.J. Metcalf, R.E. Critoph, Y. Zhong, R. Thorpe, Carbon–ammonia pairs for adsorption refrigeration applications: Ice making, air conditioning and heat pumping, Int. J. Refrig 32 (2009) 1212–1229.
[7] R. Wang, R. Oliveira, Adsorption refrigeration–An efficient way to make good use of waste heat and solar energy, Prog. Energy Combust. Sci. 32 (2006) 424–458.
[8] Y. Aristov, Concept of adsorbent optimal for adsorptive cooling/heating, Appl. Therm. Eng. 72 (2014) 166–175.
[9] B.B. Saha, K. Uddin, A. Pal, K. Thu, Emerging sorption pairs for heat pump applications: An overview, JMST, Advances (2019).
[10] H.C. Zhou, J.R. Long, O.M. Yaghi, Introduction to metal–organic frameworks, Chem. Rev. 112 (2012) 673–674.
[11] M.F. de Lange, T. Zeng, T.J.H. Vlugt, J. Gascon, F. Kapteijn, Manufacture of dense CAU-10-H coatings for application in adsorption driven heat pumps: optimization and characterization, CrystEngComm 17 (2015) 5911–5920.
[12] M.F. de Lange, K.J. Verouden, T.J. Vlugt, J. Gascon, F. Kapteijn, Adsorption-driven heat pumps: the potential of metal–organic frameworks, Chem. Rev. 115 (2015) 12205–12250.
[13] Y.K. Seo, J.W. Yoon, J.S. Lee, Y.K. Hwang, C.H. Jun, J.S. Chang, S. Wuttke, P. Bazin, A. Vimont, M. Daturi, S. Bourrelly, P.L. Llewellyn, P. Horcajada, C. Serre, G. Ferey, Energy–efficient dehumidification over hierachically porous metal–organic frameworks as advanced water adsorbents, Adv. Mater. 24 (2012) 806–810.
[14] P. Küsgens, M. Rose, I. Senkovska, H. Fröde, A. Henschel, S. Siegle, S. Kaskel, Characterization of metal–organic frameworks by water adsorption, Microporous Mesoporous Mater. 120 (2009) 325–330.
[15] X. Xia, M. Cao, Z. Liu, W. Li, S. Li, Elucidation of adsorption cooling characteristics of Zr-MOFs: Effects of structure property and working fluids, Chem. Eng. Sci. 204 (2019) 48–58.
[16] N.C. Burtch, H. Jasuja, K.S. Walton, Water stability and adsorption in metal–organic frameworks, Chem. Rev. 114 (2014) 10575–10612.
[17] P.M. Schoenecker, C.G. Carson, H. Jasuja, C.J.J. Flemming, K.S. Walton, Effect of water adsorption on retention of structure and surface area of metal–organic frameworks, Ind. Eng. Chem. Res. 51 (2012) 6513–6519.
[18] K.S. Park, Z. Ni, A.P. Côté, J.Y. Choi, R. Huang, F.J. Uribe-Romo, H.K. Chae, M. O'Keeffe, O.M. Yaghi, Exceptional chemical and thermal stability of zeolitic imidazolate frameworks, Proc. Natl. Acad. Sci. USA 103 (2006) 10186–10191.
[19] Y. Bai, Y. Dou, L.H. Xie, W. Rutledge, J.R. Li, H.C. Zhou, Zr-based metal–organic frameworks: design, synthesis, structure, and applications, Chem. Soc. Rev. 45 (2016) 2327–2367.
[20] J.P. Zhang, A.X. Zhu, R.B. Lin, X.L. Qi, X.M. Chen, Pore surface tailored SOD-type metal-organic zeolites, Adv. Mater. 23 (2011) 1268–1271.
[21] R.E. Critoph, Y. Zhong, Review of trends in solid sorption refrigeration and heat pumping technology, Proc. Inst. Mech. Eng., Part E: J. Process Mech. Eng. 219 (2004) 285–300.
[22] V. Brancato, L. Gordeeva, A. Sapienza, A. Freni, A. Frazzica, Dynamics study of ethanol adsorption on microporous activated carbon for adsorptive cooling applications, Appl. Therm. Eng. 105 (2016) 28–38.
[23] K. Thu, N. Takeda, T. Miyazaki, B.B. Saha, S. Koyama, T. Maruyama, S. Maeda, T. Kawamata, Experimental investigation on the performance of an adsorption system using Maxsorb III + ethanol pair, Int. J. Refrig 105 (2019) 148–157.
[24] M. Li, H.B. Huang, R.Z. Wang, L.L. Wang, W.D. Cai, W.M. Yang, Experimental study on adsorbent of activated carbon with refrigerant of methanol and ethanol for solar ice maker, Renew. Energy 29 (2004) 2235–2244.
[25] V. Brancato, A. Frazzica, A. Sapienza, L. Gordeeva, A. Freni, Ethanol adsorption onto carbonaceous and composite adsorbents for adsorptive cooling system, Energy 84 (2015) 177–185.
[26] L. Gordeeva, Y. Aristov, Novel sorbents of ethanol "salt confined to porous matrix" for adsorptive cooling, Energy 35 (2010) 2703–2708.
[27] M.F. de Lange, B.L. van Velzen, C.P. Ottevanger, K.J. Verouden, L.C. Lin, T.J. Vlugt, J. Gascon, F. Kapteijn, Metal–organic frameworks in adsorption–driven heat pumps: the potential of alcohols as working fluids, Langmuir 31 (2015) 12783–12796.
[28] F. Jeremias, D. Fröhlich, C. Janiak, S.K. Henninger, Water and methanol adsorption on MOFs for cycling heat transformation processes, New J. Chem. 38 (2014) 1846–1852.
[29] A. Rezk, R. Al-Dadah, S. Mahmoud, A. Elsayed, Investigation of ethanol/metal organic frameworks for low temperature adsorption cooling applications, Appl. Energy 112 (2013) 1025–1031.
[30] B.B. Saha, I.I. El-Sharkawy, T. Miyazaki, S. Koyama, S.K. Henninger, A. Herbst, C. Janiak, Ethanol adsorption onto metal organic framework: theory and experiments, Energy 79 (2015) 363–370.
[31] W. Li, X. Xia, M. Cao, S. Li, Structure–property relationship of metal–organic frameworks for alcohol-based adsorption-driven heat pumps via high-throughput computational screening, J. Mater. Chem. A 7 (2019) 7470–7479.
[32] W. Li, X. Xia, S. Li, Large-scale evaluation of cascaded adsorption heat pumps based on metal/covalent–organic frameworks, J. Mater. Chem. A (2019) 25010–25019.
[33] X. Feng, X. Ding, D. Jiang, Covalent organic frameworks, Chem. Soc. Rev. 41 (2012) 6010–6022.
[34] J. Pérez-Carvajal, G. Boix, I. Imaz, D. Maspoch, The imine-based COF TpPa-1 as an efficient cooling adsorbent that can be regenerated by heat or light, Adv. Energy Mater. 9 (2019) 1901535.
[35] C.S. Diercks, O.M. Yaghi, The atom, the molecule, and the covalent organic framework, Science 355 (2017) 6328.
[36] P.B.S. Rallapalli, M.C. Raj, S. Senthilkumar, R.S. Somani, H.C. Bajaj, HF-free synthesis of MIL-101(Cr) and its hydrogen adsorption studies, Environ. Prog. Sustain. Energy 35 (2016) 461–468.
[37] B.J. Smith, W.R. Dichtel, Mechanistic studies of two-dimensional covalent organic

frameworks rapidly polymerized from initially homogenous conditions, J. Am. Chem. Soc. 136 (2014) 8783–8789.
[38] J. Cravillon, S. Münzer, S.-J. Lohmeier, A. Feldhoff, K. Huber, M. Wiebcke, Rapid room-temperature synthesis and characterization of nanocrystals of a prototypical zeolitic imidazolate framework, Chem. Mater. 21 (2009) 1410–1412.
[39] Q. Wang, D. Shen, M. Bülow, M. Lau, S. Deng, F.R. Fitch, N.O. Lemcoff, J. Semanscin, Metallo-organic molecular sieve for gas separation and purification, Microporous Mesoporous Mater. 55 (2002) 217–230.
[40] K.C. Ng, M. Burhan, M.W. Shahzad, A.B. Ismail, A universal isotherm model to capture adsorption uptake and energy distribution of porous heterogeneous surface, Sci. Rep. 7 (2017) 10634.
[41] B. Mu, K.S. Walton, Thermal analysis and heat capacity study of metal–organic frameworks, J. Phys. Chem. C 115 (2011) 22748–22754.
[42] M. Pons, F. Meunier, G. Cacciola, R.E. Critoph, M. Groll, L. Puigjaner, B. Spinner, F. Ziegler, Thermodynamic based comparison of sorption systems for cooling and heat pumping, Int. J. Refrig 22 (1999) 5–17.
[43] H. Kummer, M. Baumgartner, P. Hügenell, D. Fröhlich, S.K. Henninger, R. Gläser, Thermally driven refrigeration by methanol adsorption on coatings of HKUST-1 and MIL-101(Cr), Appl. Therm. Eng. 117 (2017) 689–697.
[44] L.M. Lanni, R.W. Tilford, M. Bharathy, J.J. Lavigne, Enhanced hydrolytic stability of self-assembling alkylated two-dimensional covalent organic frameworks, J. Am. Chem. Soc. 133 (2011) 13975–13983.
[45] M.H. Bagheri, S.N. Schiffres, Ideal Adsorption isotherm behavior for cooling applications, Langmuir 34 (2018) 1908–1915.
[46] J. Canivet, J. Bonnefoy, C. Daniel, A. Legrand, B. Coasne, D. Farrusseng, Structure–property relationships of water adsorption in metal–organic frameworks, New J. Chem. 38 (2014) 3102–3111.
[47] F. Jeremias, A. Khutia, S.K. Henninger, C. Janiak, MIL-100(Al, Fe) as water adsorbents for heat transformation purposes–a promising application, J. Mater. Chem. 22 (2012) 10148–10151.